

# Photoemission study of electronic structures of disordered Ni-Pt and Cu-Pt alloys

Tschang-Uh Nahm,\* Jae-Young Kim, and S.-J. Oh  
*Department of Physics, Seoul National University, Seoul 151-742, Korea*

S.-M. Chung  
*Department of Physics, Pohang University of Science and Technology, Pohang 790-784, Korea*

J.-H. Park<sup>†</sup> and J. W. Allen  
*Department of Physics, University of Michigan, Ann Arbor, Michigan 48109-1120*

K. Jeong  
*Department of Physics, Yonsei University, Seoul 120-749, Korea*

Sehun Kim  
*Department of Chemistry and Center for Molecular Science, Korea Advanced Institute of Science and Technology, Taejon 373-1, Korea*

(Received 22 May 1995; revised manuscript received 17 April 1996)

The valence-band photoemission spectra of disordered  $\text{Ni}_x\text{Pt}_{1-x}$  and  $\text{Cu}_x\text{Pt}_{1-x}$  alloys have been measured with synchrotron radiation. Using the Cooper minimum phenomenon of the Pt  $5d$  electron photoionization cross section and taking the matrix-element effect into account, we obtain experimental partial spectral weights (PSW's) of each constituent. For the Ni-rich Ni-Pt alloys, we find substantial weights of the Pt states near the Fermi level, which are believed to be responsible for the Pt local magnetic moment. The comparison with the theoretical calculations in this case shows the importance of both relativistic effect and the self-consistent-field treatment. For the Cu-rich Cu-Pt alloys, we find that due to the strong hybridization Cu  $3d$  and Pt  $5d$  states form a common band. This calls into question the conclusion of the early photoemission study that Pt impurity forms a virtual bound state in the Cu host. [S0163-1829(96)07135-4]

## I. INTRODUCTION

It has long been an interesting subject to predict and understand the electronic structures of disordered alloys. Theoretical approaches have achieved great success in the last decade through the development of the coherent-potential approximation (CPA). Korringa-Kohn-Rostoker (KKR) CPA has predicted the electronic structure of disordered alloys, which has been confirmed in many cases by experiments, especially the photoelectron spectroscopy (PES). In this paper, we present the results of a photoemission study on two alloy systems, disordered Ni-Pt alloys and Cu-rich Cu-Pt alloys, and discuss their electronic structures in relation to physical properties and theoretical band calculations. Below, we will first briefly review some issues pertinent to these Pt alloy systems and discuss our motivations for the present study.

### A. Ni-Pt alloys

The disordered Ni-Pt alloy system has received much attention because of its magnetic<sup>1-3</sup> and catalytic behaviors.<sup>4,5</sup> Neutron scattering studies and magnetization measurement<sup>2,3</sup> of this alloy system showed that the average magnetic moment decreases as the Pt concentration is increased, and finally the alloy becomes paramagnetic with more than 58 at. % Pt, which is called the critical concentration. This behavior is similar to those of many Ni nonmagnetic metal

alloys, but this system is different from such alloy systems as Ni-Cu in that the Pt atomic site also has the magnetic moment which is about half that of the Ni atomic site.<sup>2,3</sup> The concentration dependence of the Curie temperature is different between disordered and ordered phases, and the lower Curie temperature of the ordered phase makes NiPt paramagnetic, while  $\text{Ni}_{50}\text{Pt}_{50}$  is ferromagnetic below about 150 K.<sup>6</sup>

There also has been a great deal of theoretical and experimental works on the determination of the surface composition of Ni-Pt alloys in order to elucidate its chemisorption and catalytic behaviors. Recent experimental works using various techniques such as x-ray photoemission spectroscopy (XPS),<sup>4</sup> Auger electron spectroscopy,<sup>7</sup> low-energy electron diffraction,<sup>8,9</sup> and ion scattering spectroscopy<sup>10,11</sup> led to the general consensus that Ni-Pt alloy system forms sandwiched structures in which monolayers of the Pt and the Ni enrichment alternate. More interesting was the observation of face-related segregation reversal, which led to the conclusion that the segregation of a polycrystalline surface would depend on the distribution of crystal faces exposed by grains.<sup>9</sup>

The electronic structure of Ni-Pt alloy system is not yet fully understood because of the theoretical difficulty in the simultaneous treatment of relativistic effects and self-consistency in site potentials in the CPA method. Early calculation which employed model  $d$  density of states (DOS) to explain the magnetic moment measurement was far from the real situation.<sup>12</sup> The most comprehensive work showing the density of states as a function of composition is probably the fully relativistic KKR-CPA calculation by Staunton *et al.*,<sup>13</sup>

but unfortunately it does not take account of self-consistency in site potentials and predicts lower DOS at the Fermi level than the XPS valence spectra show.<sup>14</sup> Self-consistent field (SCF) KKR-CPA and its atomic-sphere approximation have been used<sup>15,16</sup> to calculate the ordering and the alloy formation energy of NiPt, but they are only nonrelativistic or scalar relativistic results and are available only for equiatomic Ni<sub>50</sub>Pt<sub>50</sub>. For the ordered alloys SCF linear muffin-tin orbitals (LMTO) calculation was reported for Ni<sub>3</sub>Pt and NiPt<sub>3</sub>,<sup>17</sup> but it was also scalar relativistic. In addition to these problems in the comparison of photoemission spectra with band calculations, Ni 3*d* states experience strong electron correlation effect which results in the narrowed valence bandwidth and the so-called 6 eV satellite.<sup>18</sup>

The earlier photoelectron spectroscopy studies<sup>14,19</sup> mainly focused on the core level spectroscopy using XPS. Shevchik and Bloch<sup>14</sup> concluded from their measurement of core level shifts that there is charge transfer from Pt to Ni, but Choi *et al.* showed that the intraatomic charge redistribution is more important than the interatomic charge redistribution between Pt and Ni atoms.<sup>19</sup> The valence-band PES spectra of both studies, however, gave little information on the partial DOS of each component because of the lack of the prominent structures which can be used to identify its parentage. In fact, Choi *et al.* compared the weighted sum of pure metal valence-band PES spectra with those of alloys, and found reasonable agreement for the whole composition. This had also been predicted by the KKR-CPA result for Pt-rich alloys,<sup>13</sup> where the partial DOS's of both constituents change little for the compositions of 30, 40, and 50 at. % of Ni. But the band calculation of Ref. 17 on ordered alloys makes this conclusion somewhat doubtful, because the Pt partial DOS changes much in its shape between Ni<sub>3</sub>Pt and NiPt<sub>3</sub>. Hence the partial spectral weight (PSW) of each component must be correctly extracted from the PES spectra to compare with theoretical predictions, which is one of the main subjects of this paper.

## B. Cu-Pt alloys

The study of Cu-Pt alloy systems is a natural extension of the Ni-Pt alloy study, since Cu is the next element to Ni in the periodic table. Ni is a transition metal element with the unfilled 3*d* shell, while Cu belongs to noble metals with the (nominally) filled 3*d* band, hence it would be interesting to see the difference of the electronic structures when they form alloys with Pt. In fact, transition metal alloys with noble metals have been most extensively studied among disordered alloy systems, one reason being that the magnetic behavior of the transition metal impurity is expected to be easily interpreted by the localized virtual bound state picture. However, recent theoretical calculations predicted rather strong hybridization between impurity states and the host band for some systems,<sup>20</sup> which called into question the adequacy of a simple model treating the transition metal impurity state as localized. One famous and most extensively studied example is the Pd impurity in the Cu host. Early photoemission studies argued for the existence of the virtual bound state,<sup>21–23</sup> while most calculations both with and without the lattice relaxation predicted a common-band behavior.<sup>24</sup> This contro-

versy has been resolved recently by considering the matrix-element effect (binding energy dependence of photoionization cross section) of Pd in the interpretation of PES experimental results,<sup>25</sup> and we have suggested that the Pd impurity states in the Cu host do form a common band although it may be difficult to observe by photoemission experiment because of the low Pd cross section at the bottom of the band.

The existence of the Pt virtual bound state in Pt diluted Cu-Pt alloys is also very doubtful considering the hybridization between the two elements, although it has been suggested in a previous PES study.<sup>22</sup> First, the hopping integral between the Pt 5*d* and the Cu 3*d* states is 1.16 times larger than that between the Pd 4*d* and the Cu 3*d* states according to Harrison's scheme<sup>26</sup> because the Pt 5*d* states are more extended. This is true even if the local lattice relaxation effect is included, since the expansion of the lattice around Pt impurity is comparable to that of Pd impurity in the Cu host.<sup>27</sup> Second, the binding energies ( $E_B$ ) of the Pd and Pt impurity levels are expected to be nearly the same. As a first approximation, the impurity levels in the Cu host can be estimated by the core level binding energies assuming rigid behavior between the core level and the valence binding energies. From the measured Pt 4*f* binding energy of Cu-Pt alloys<sup>28</sup> and the Pd 3*d* binding energy shift of the Pd-diluted Cu-Pd alloys,<sup>21</sup> we can infer that the centroid of the Pt 5*d* and the Pd 4*d* levels in the Cu 3*d* host will both be around  $E_B \approx 4$  eV, which is well inside the Cu 3*d* band. Therefore, we can conclude that the hybridization mixing between the Pt impurity states and the Cu host band is stronger than that between the Pd impurity states and the Cu host band. This means that if the Pd 4*d* impurity states form a common band, the Pt impurity states must also form the common band, not a virtual bound state. Hence it is interesting to study the electronic structure of Cu-Pt alloys more carefully.

There have been only a few photoemission works on Cu-Pt alloys compared with the extensively studied Cu-Pd alloy case. The early XPS work gave little information about the valence band due to the inadequate energy resolution.<sup>28</sup> More recent ultraviolet PES (UPS) work<sup>22</sup> on Pt- and Pd-diluted alloys with He I lines ( $h\nu = 21.2$  eV) concluded that the Pt and Pd impurity levels form virtual bound states in the Cu host, but the underlying assumption in the analysis that the matrix element of Pt be similar to that of Cu may be unjustified. Furthermore, it is not clear whether the spectra with He I lines represent the total density of states, because with photon energies less than about 40 eV, one generally cannot obtain full information about the angle-integrated DOS.<sup>29</sup>

The DOS calculation on Cu-Pt alloys with KKR-CPA has been done only for 85, 50, and 29 at. % Pt alloys.<sup>30,31</sup> Therefore, the direct comparison between the UPS result of dilute limit<sup>22</sup> and the band calculation is not possible. But we can get some trend and hint on the electronic structure of the Pt impurity in the Cu host. As the Cu content increases, the DOS at the Fermi level is decreased and the deeper binding energy structure moves away from the bottom of the Cu band while gaining weight. In Cu<sub>71</sub>Pt<sub>29</sub>, the centroid binding energy of the Pt partial DOS is about 4 eV. So it is

questionable that the partial DOS of the Pt impurity in the Cu host forms a narrow virtual bound state around  $E_B \approx 2$  eV, as claimed in Ref. 22.

In this paper, we report the valence-band PES spectra of  $\text{Ni}_x\text{Pt}_{1-x}$  alloys of various composition ( $x=0.10, 0.30, 0.50, 0.75, 0.898$ ;  $x=0.898$  will be designated as 0.90 henceforth) and Cu-rich  $\text{Cu}_x\text{Pt}_{1-x}$  ( $x=0.5, 0.75, 0.9$ ) alloys with variable incident photon energy using synchrotron radiation. By making use of the Cooper minimum phenomenon of the Pt  $5d$  states, we deduce the PSW's of Ni, Cu, and Pt separately. We then compare them with theoretical calculations to assess the validity of the KKR-CPA calculation, and also gain some insight on the question whether Pt  $5d$  states in the Pt-diluted alloy form a virtual bound state or not.

The organization of this paper is as follows. Following this Introduction, the experimental details are described in Sec. II. In Sec. III, the results of a PES study on  $\text{Ni}_x\text{Pt}_{1-x}$  alloys will be discussed. The results on  $\text{Cu}_x\text{Pt}_{1-x}$  alloys will then be presented in Sec. IV. The paper concludes with a brief summary in Sec. V.

## II. EXPERIMENT

The polycrystalline samples of  $\text{Ni}_x\text{Pt}_{1-x}$  ( $x=0.10, 0.30, 0.50, 0.75, \text{ and } 0.90$ ) alloys and  $\text{Cu}_x\text{Pt}_{1-x}$  ( $x=0.5, 0.75, \text{ and } 0.9$ ) alloys were prepared by arc melting of two constituents in an atmosphere of argon on a water-cooled copper hearth. For the Ni-Pt alloys, the homogenizing anneal at  $1200 \pm 25$  °C was performed afterwards for 27 h. The x-ray diffraction measurements confirmed homogeneous face-centered-cubic solid solutions for both samples. The Ni-Pt alloy system has well-defined ordered phases  $\text{Ni}_3\text{Pt}$  and  $\text{NiPt}$  which have  $L1_2$  and  $L1_0$  structures below 580 and 645 °C, respectively,<sup>6</sup> but no ordered phase was observed in our samples.

The valence-band photoemission spectra were taken at National Synchrotron Light Source (NSLS) Beamline U4A of Brookhaven National Laboratory equipped with a 6 m/160° toroidal grating monochromator. The total resolution at the Fermi level was less than 0.3 eV in full width at half maximum (FWHM) for photon energies below 160 eV. At higher photon energies, the resolution was broadened to  $\sim 0.45$  eV due to the low photon flux. The incident photon energy ranged from 40 eV to 200 eV. The measurement of photocurrents was performed by Vacuum Scientific Workshop (VSW) HA100 concentric hemispherical analyzer with single channel electron multiplier under the base pressure of low  $10^{-10}$  torr.

To remove the contaminations at the surface, the samples were sputtered with 1.0 keV neon or argon ions for about 20 min. Since sputtering generally gives damaged surfaces which are somewhat amorphous, subsequent annealing at the temperature of about 240 °C for 20 min was done to ensure the crystalline sample surface. This procedure was repeated until we obtained clean surfaces.

## III. RESULTS AND DISCUSSION ON Ni-Pt ALLOYS

### A. Raw spectra

Figure 1 shows the raw PES spectra of Ni-Pt alloys and

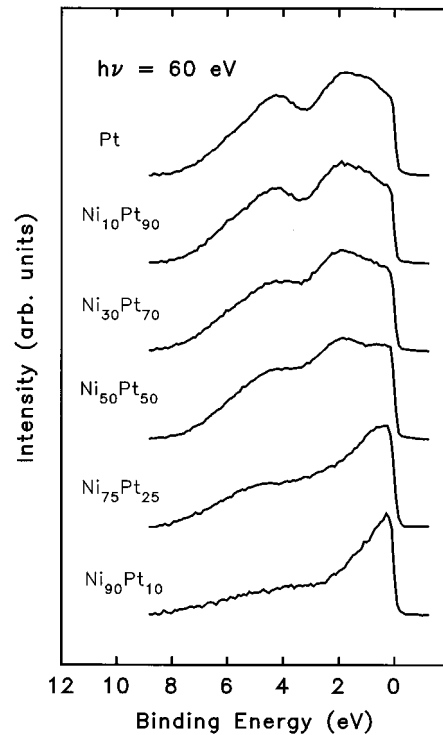


FIG. 1. Valence-band photoemission spectra of Pt,  $\text{Ni}_{10}\text{Pt}_{90}$ ,  $\text{Ni}_{30}\text{Pt}_{70}$ ,  $\text{Ni}_{50}\text{Pt}_{50}$ ,  $\text{Ni}_{75}\text{Pt}_{25}$ , and  $\text{Ni}_{90}\text{Pt}_{10}$  with photon energy  $h\nu = 60$  eV, normalized to have the same maximum heights. The inelastic background is removed and the analyzer transmission function is corrected assuming  $1/E$  behavior.

pure Pt metal with photon energy  $h\nu = 60$  eV, where the calculated atomic cross section ratio<sup>32</sup> between Ni  $3d$  and Pt  $5d$  states is 0.8. The electron analyzer transmission function has been corrected assuming  $1/E$  behavior, and the inelastic scattering background has been removed. We can see that as the Ni content increases, so does the spectral intensity at the Fermi level due to the Ni  $3d$  emission. Also, the total bandwidth becomes smaller and the depth of a dip related to the spin-orbit splitting of the Pt PSW diminishes. But it is difficult to separate out Ni and Pt partial DOS's because they overlap each other.

Figure 2 shows the raw spectra of Ni-Pt alloys and pure metals at  $h\nu = 130$  eV, where the calculated atomic cross section ratio<sup>32</sup> between Ni  $3d$  and Pt  $5d$  is 13.7 and Ni  $3d$  states are expected to dominate the spectra. However, this theoretical cross section ratio is much overestimated as we will show below. In this figure we can see that as the Ni content is decreased from pure Ni down to  $\text{Ni}_{50}\text{Pt}_{50}$ , the bandwidth of the Ni-related spectral weight is reduced. This probably comes from the weaker hybridization between Ni  $3d$  states in alloys due to the dilated Ni atomic site (the lattice constant is 3.52 Å and 3.92 Å for pure Ni and Pt metals, respectively). But it is not clear whether the Ni PSW's of Pt-rich alloys have further reduced bandwidth or not, since the hybridization between Ni  $3d$  and Pt  $5d$  states may broaden the Ni partial DOS somewhat.

### B. Photoionization cross section

In order to separate out the PSW's of each element quantitatively, we make use of the Cooper minimum phenomenon

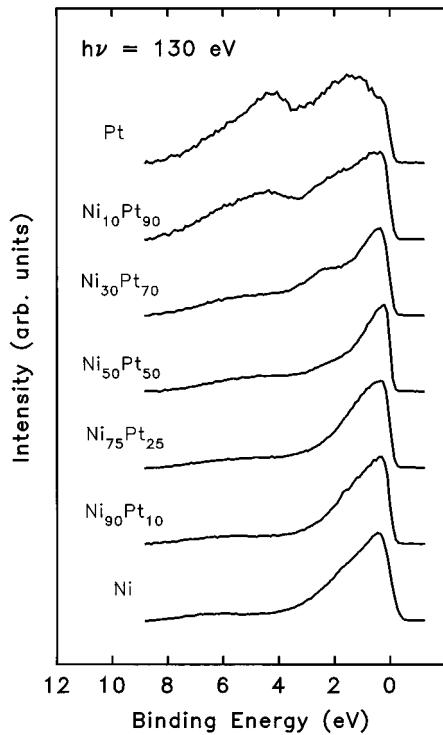


FIG. 2. Photoemission spectra of Pt, Ni<sub>10</sub>Pt<sub>90</sub>, Ni<sub>30</sub>Pt<sub>70</sub>, Ni<sub>50</sub>Pt<sub>50</sub>, Ni<sub>75</sub>Pt<sub>25</sub>, Ni<sub>90</sub>Pt<sub>10</sub>, and Ni with photon energy  $h\nu=130$  eV. Other details are the same as in Fig. 1.

of the Pt 5d level photoionization cross section.<sup>32</sup> The procedure determining experimental values of the photoionization cross section ratio as a function of the incident photon energy is described in detail in our previous works.<sup>25</sup> It is based on the fact that the intensity ratios of the valence-band PES spectra taken at different photon energies are proportional to their cross section ratios. The proportionality constant is fixed by setting the intensity ratio of core levels measured with XPS equal to the atomic cross section calculation,<sup>32</sup> since the cross sections of core levels are not expected to change much from their atomic values even in solids. For Ni-Pt alloys, we used the Pt 4f (binding energy  $E_B=71$  eV for  $f_{5/2}$ ) and the Ni 3p ( $E_B=67$  eV for  $p_{3/2}$ ) core levels, which have similar kinetic energies so that the escape depth would also be similar. The experimental cross section ratio between Ni 3d and Pt 5d states thus determined as a function of the photon energy is shown in Fig. 3 along with the calculated atomic values of Ref. 32.

The overall trend is slightly different between experiment and theory. The atomic calculation predicts a rapid increase of the cross section ratio up to  $h\nu \approx 150$  eV, but the experimental data show a smaller value of the ratio which increases rather slowly. As a result, the cross section ratio between the Ni 3d and the Pt 5d states at  $h\nu = 130$  eV is greatly reduced from the calculated atomic value 13.7 to the experimental value of 2.5. Similar, although a little smaller in magnitude, discrepancy between theory and experiment is observed for the cross section ratio between Cu 3d and Au 5d states,<sup>33</sup> as well as that between Cu 3d and Pt 5d states (see Sec. IV A), and we can ascribe these changes to the solid state effect. This will affect partial DOS's deduced from these spectra

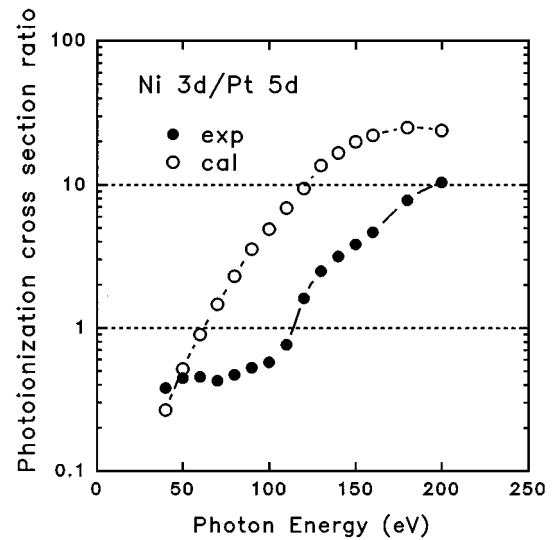


FIG. 3. Photoionization cross section ratio of the Ni 3d to that of the Pt 5d states at  $h\nu = 40\text{--}200$  eV, both the experimental solid state (filled circles) and the calculated atomic values (open circles) (Ref. 32). The experimental ratio between Ni 3d and Pt 5d states is less than half that of the calculated atomic value at around  $h\nu \approx 110$  eV.

and we note again the importance of the experimental determination of the cross section ratio.

### C. Partial spectral weights

The procedure used to obtain the PSW of binary alloys is also described in Ref. 25. It assumes no change in the photoionization matrix element of a constituent between pure metal and alloys. But the dependence of the matrix element on the photon energy and on the binding energy is correctly included. Since the experimental value of  $\sigma_{3d}^{\text{Ni}}/\sigma_{5d}^{\text{Pt}}$  is 2.5 at  $h\nu=130$  eV, we can regard the PES spectra at that photon energy as the Ni PSW's as a first step. Using the measured cross section ratio and the divided spectra of pure Ni at different photon energies (130 and 60 eV) representing the change in the matrix element, we can obtain the Pt PSW's at  $h\nu=60$  eV. With these Pt PSW's, more correct Ni PSW's at  $h\nu=130$  eV can be determined with similar method. Iterations of 3 or 4 times are enough to obtain the converged results.

In this procedure, we should take into account the surface segregation phenomena. As discussed in the Introduction, it is well known that the surface composition of the polycrystalline Ni-Pt alloys is different from the bulk, and it may depend on the surface treatment. Since the inelastic electron mean free path of photoelectrons at soft x-ray regime is very short, we should use the surface compositions of the alloys to obtain correct PSW's. However, we expect the surface composition of our samples to be somewhat different from that of the equilibrated surfaces annealed at temperatures higher than 870 K, because our annealing temperature was only 240 °C. Recent scanning-tunneling microscope measurement on Ni<sub>75</sub>Pt<sub>25</sub>(111) single crystal<sup>34</sup> showed that the dislocations due to the preferential sputtering and the recoil mixing do not disappear even after annealing if the temperature is

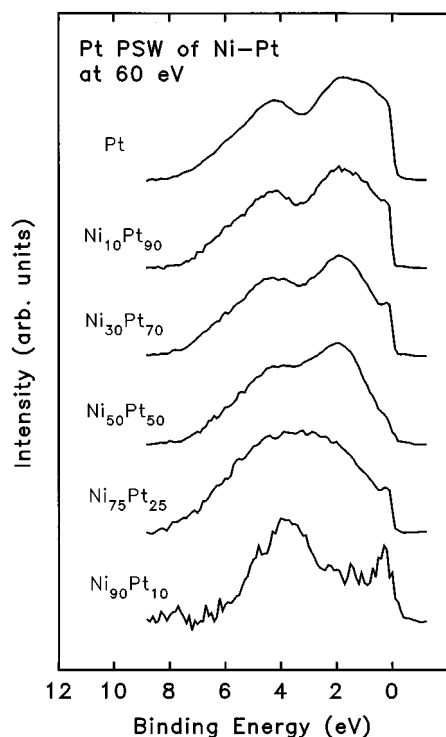


FIG. 4. Experimental Pt partial spectral weights of Ni-Pt alloys at  $h\nu = 60$  eV using the experimentally determined cross section ratio and including the Pt enrichment effect at the surface.

lower than about 870 K. Therefore, we will use here the surface composition of the sputtered Ni-Pt alloys, which shows Pt-enriched surfaces throughout the whole compositions.<sup>35</sup> The reason is that we observed the valence band spectra after annealing at 240 °C for 20 min were virtually the same as those of the sputtered surfaces, showing only minute reduction in the intensity of the Pt-related structures.

The solid lines of Fig. 4 show the PSW's of Pt at  $h\nu = 60$  eV, obtained by assuming the surface composition of 17, 35, 62, 78, and 92 % of Pt for alloys with the bulk composition of 10, 25, 50, 70, and 90 % of Pt, respectively.<sup>35</sup> These surface compositions were determined with the Auger lines of Ni (848 eV) and Pt (239 eV) for sputtered surfaces,<sup>35</sup> and it may be that the surface enrichment is slightly underestimated because these Auger electrons have larger electron inelastic mean free paths than the photoelectrons in our spectra at  $h\nu=60$  eV. But this underestimation is expected to be compensated by the slight reduction of the Pt-related spectral weights after annealing, and in any event such a small error in the surface composition does not affect the experimental PSW's seriously.

The Pt PSW's of the ferromagnetic alloys  $\text{Ni}_{75}\text{Pt}_{25}$  and  $\text{Ni}_{90}\text{Pt}_{10}$  have appreciable amount of the Pt states at the Fermi level, probably due to strong mixing with the Ni 3d states. This is in accord with the band calculation for ordered  $\text{Ni}_3\text{Pt}$  which shows a large amount of the Pt related states at the Fermi level.<sup>17</sup> These states are of great importance in understanding the magnetic property of Ni-Pt alloys. As pointed out by Williams *et al.*,<sup>36</sup> some metallic magnetism can be understood when one considers the covalent bonding in band formation instead of the Stoner magnetism. The local

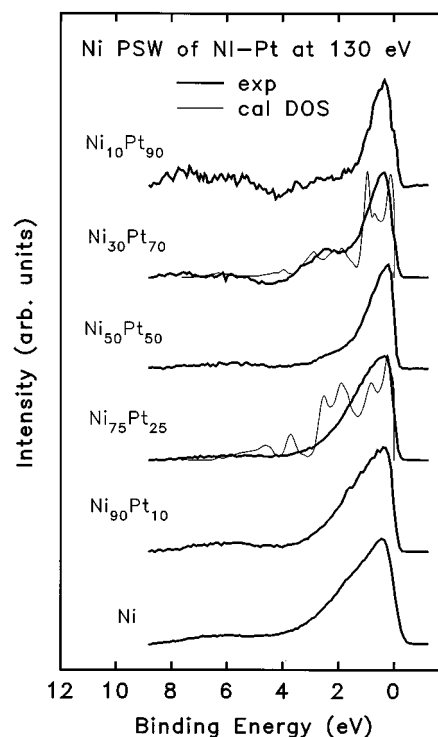


FIG. 5. Experimental Ni partial spectral weights of Ni-Pt alloys at  $h\nu = 130$  eV using the experimentally determined cross section ratio. The calculated Ni partial DOS of ordered  $\text{NiPt}_3$  and  $\text{Ni}_3\text{Pt}$  from Ref. 17 (thin lines) are shown for comparison.

magnetic moments of Pt in the Ni-rich Ni-Pt alloys also come from the covalent bonding which splits the Pt states into the higher binding bonding states and the lower binding antibonding states hybridized with the Ni 3d band near the Fermi level. The higher binding states at  $E_B \sim 4$  eV participate little in the local magnetic moment of Pt because of small degree of mixing with the ferromagnetic Ni 3d band. Hence the Pt states at the Fermi level which mixes strongly with the Ni 3d states give rise to the local moment of the Pt site in Ni-Pt alloys. For Ni-Cu alloys, this kind of magnetic moment does not occur due to the relatively weak hybridization which is insufficient to form mixed states composed of the Cu 3d and the Ni 3d states.

In Fig. 5, we present the Ni PSW's at  $h\nu=130$  eV, and also show the calculated Ni partial DOS (Ref. 17) of  $\text{Ni}_3\text{Pt}$  and  $\text{NiPt}_3$  for comparison. Since the Ni 3d band is strongly influenced by many-body effects, the width of the Ni PSW is smaller than that of band calculations. As the Ni content is decreased, the Ni 3d bandwidth gets smaller down to 50 at. % of Ni, but in  $\text{Ni}_{30}\text{Pt}_{70}$  the Ni PSW has more weight at around 2.5 eV than that of  $\text{Ni}_{50}\text{Pt}_{50}$ . This probably comes from the increased mixing between Ni 3d and Pt 5d states as seen in the calculation of ordered  $\text{NiPt}_3$  (Ref. 17).

#### D. Comparison with band calculation

In this section we will discuss the comparison of our experimental PSW's with the results of various band structure calculations. Although the equilibrated Ni-Pt alloy surface annealed at temperature higher than 870 K show sandwich

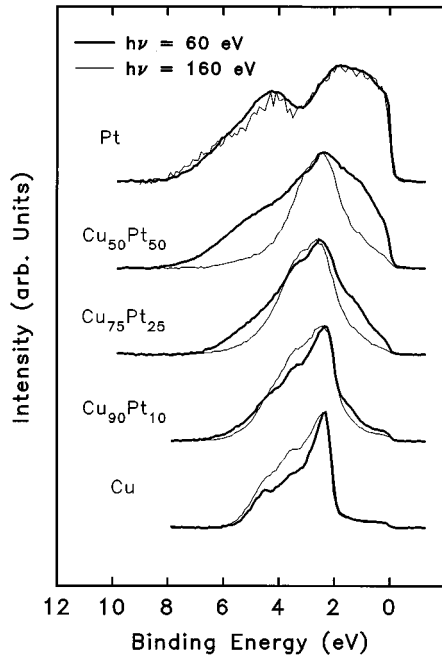


FIG. 6. Valence-band photoemission spectra of Pt,  $\text{Cu}_{50}\text{Pt}_{50}$ ,  $\text{Cu}_{75}\text{Pt}_{25}$ ,  $\text{Cu}_{90}\text{Pt}_{10}$ , and Cu with the photon energy  $h\nu=60$  eV (thick lines) and 160 eV (thin lines) from sputter-annealed samples.

structure, our sample surfaces annealed at lower temperature would remain random and disordered as explained above, so the comparison with CPA calculations would be meaningful.

The main disagreement between the experiment and the non-SCF relativistic CPA calculation<sup>13,37</sup> is the position of the Ni 3*d* states in the Ni-diluted alloys. The theory predicts deeper binding Ni 3*d* band resulting in very low Ni 3*d* DOS at the Fermi level, which clearly is not the case as seen in Fig. 5. This is probably due to the non-self-consistent-field treatment of site potentials in the calculation, which sometimes assigns wrong resonance energies to the electronic states, especially when the charge transfer effect is significant. The fact that non-SCF calculation poorly predicts the experimental PSW implies the importance of the interatomic charge redistribution effect between Ni and Pt atoms in Ni-Pt alloys, as recently suggested.<sup>16</sup> The electron correlation effect in the Ni 3*d* band may also contribute to this discrepancy between theory and experiment, but we do not believe it is a major factor. The reason is that in the case of Ni metal the main effect of the self-energy due to the electron correlation was found to be the reduction of the bandwidth and the appearance of a valence-band satellite.<sup>38</sup> On the other hand in the present case the major discrepancies are the position of the main *d* band resonance and the density of states at the Fermi level where the self-energy effect should be small. In this respect, it is interesting to note that the recent SCF scalar-relativistic calculation<sup>16</sup> shows the total DOS of  $\text{Ni}_{50}\text{Pt}_{50}$  which is rather similar to our spectra at 110 eV where experimental  $\sigma_{3d}^{\text{Ni}}/\sigma_{5d}^{\text{Pt}}$  is 0.8, except for the narrowed Ni 3*d* bandwidth and the absence of the spin-orbit splitting. However Ref. 16 unfortunately gives no partial DOS that can be compared with our experimental PSW. We might also mention that the comparison with the calculations for or-

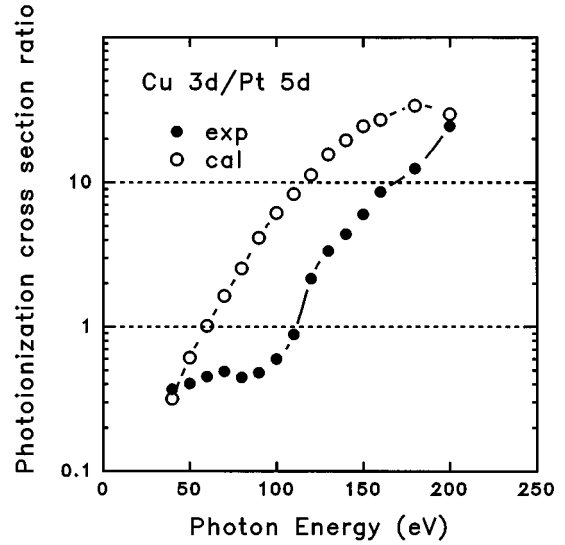


FIG. 7. Photoionization cross section ratio between the Cu 3*d* and the Pt 5*d* states in pure metals [open circles represent the calculated atomic values (Ref. 32)]. Due to the Cooper minimum phenomenon of the Pt 5*d* states around 200 eV, the ratio increases steadily.

dered alloys  $\text{Ni}_3\text{Pt}$  and  $\text{NiPt}_3$  in Ref. 17 shows reasonable agreements overall, except for some discrepancies in the detailed structures.

#### IV. RESULTS AND DISCUSSION ON Cu-Pt ALLOYS

##### A. Photoemission spectra and photoionization cross section

The raw photoemission spectra of Cu-Pt alloys at  $h\nu=60$  eV and 160 eV are shown in Fig. 6. The calculated atomic cross section ratios<sup>32</sup> between the Cu 3*d* and the Pt 5*d* states are 1 and 27 at these photon energies, respectively, and we can regard the spectra at  $h\nu=160$  eV as the Cu PSW's at that photon energy. The comparison of the spectra at these two photon energies for  $\text{Cu}_{75}\text{Pt}_{25}$  clearly shows that the Pt PSW at  $h\nu=60$  eV extends to  $E_B \approx 7$  eV. For the Pt PSW of  $\text{Cu}_{90}\text{Pt}_{10}$ , we can see that the structure near 2 eV is obviously Pt 5*d* related, but we must also note the structure around  $E_B \approx 5$  eV of the spectra at  $h\nu=60$  eV. Since the spectral weight of the Cu partial DOS at that binding energy region is rather small, it may indicate that higher binding energy structures of  $\text{Cu}_{90}\text{Pt}_{10}$  include substantial amount of the Pt 5*d* states.

Figure 7 shows the experimental cross section ratio between Cu 3*d* and Pt 5*d* states as a function of the incident photon energy obtained by the procedure described in Sec. III B. Here, we used the Pt 4*f* (71.3 eV for  $f_{7/2}$ ) and the Cu 3*p* (77 eV for  $p_{3/2}$ ) levels to fix the proportionality constant. The result of the atomic photoionization cross section calculation<sup>32</sup> is also shown in the figure for comparison. The atomic calculation predicts rapid increase of the cross section ratio between the Cu 3*d* and the Pt 5*d* electrons up to  $h\nu \approx 150$  eV, but the experimental results show smaller values which increase rather slowly. It can be seen that the

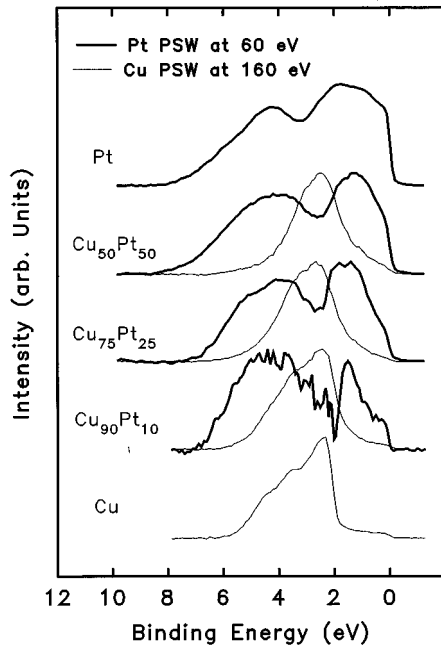


FIG. 8. Experimental Pt and Cu partial spectral weights of Cu-Pt alloys at  $h\nu=160$  eV and 60 eV, respectively, using the experimentally determined cross section ratio assuming no surface segregation. Note the large Pt spectral weights at the bottom of the band, which indicate the absence of the virtual bound state behavior of Pt  $5d$  states.

experimental cross section ratio varies by the factor of 10 between  $h\nu=60$  eV and 160 eV.

### B. Partial spectral weights

Due to the large value of cross section ratio at 160 eV, the spectra can be regarded in the first approximation as the Cu PSW's at that photon energy. Following the procedure described in Ref. 25, the Pt PSW at 60 eV can be determined with the measured cross section ratio and the divided spectra representing the change in the matrix elements of pure Cu between 160 and 60 eV. This approximate Pt PSW at 60 eV is then transferred to 160 eV, and then a better Cu PSW at 160 eV can be obtained by a similar method. This process is iterated until we obtain self-consistent results.

In this process we have to take into account the difference of alloy compositions at the surface compared with the bulk, since the inelastic electron mean free path at soft x-ray regime is very short. It was reported using Auger electron spectroscopy<sup>39</sup> (AES) that polycrystalline Cu-Pt alloys have sandwiched structures when thermally equilibrated. The uppermost layer is Cu rich, which was also confirmed by ion scattering spectroscopy work.<sup>40</sup> On the other hand, sputtered alloys were all reported to have Pt enriched surfaces<sup>35</sup> in contrast to the thermally equilibrated surfaces. The sample surfaces we used in our present study were prepared by sputtering and annealing. However, the annealing temperature was rather low just to cure the amorphous state of the sputtered surface, and so it is not expected to produce the thermodynamically equilibrated surfaces since dislocations made by ion bombardment are not generally removed by the low-

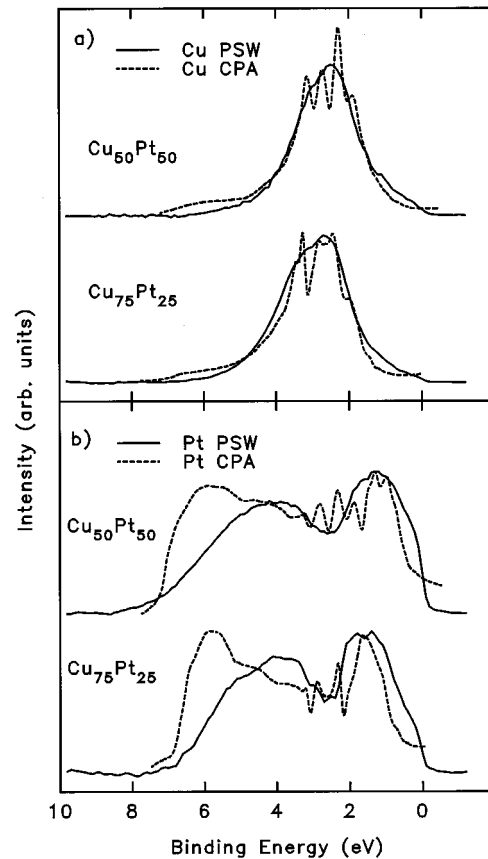


FIG. 9. Comparison of the experimental (a) Cu and (b) Pt partial spectral weights of  $\text{Cu}_{50}\text{Pt}_{50}$  and  $\text{Cu}_{75}\text{Pt}_{25}$  with the KKR-CPA calculations (Ref. 30) for  $\text{Cu}_{50}\text{Pt}_{50}$  and  $\text{Cu}_{71}\text{Pt}_{29}$ . Solid lines are experimentally determined partial spectral weights, and dashed lines show the partial DOS predicted by CPA calculations. The Fermi levels of the theoretical curves are shifted by 0.6 eV to align the Cu spectral features.

temperature annealing as mentioned earlier.<sup>41</sup> Still, during this low temperature annealing we observed some change in the surface composition. After annealing, structures due to the Pt states were found to be reduced, which implies the Cu enrichment relative to the sputtered surfaces. Judging from this intensity change, the amount of the Cu enrichment after the low-temperature anneal seems to restore roughly the original bulk composition from the Pt enriched sputtered surface. Hence in our analysis we assumed the bulk composition of alloys. This assumption was justified *a posteriori* by checking whether the sum of the resulting Cu and Pt PSW's with the reported Pt enriched composition<sup>35</sup> reproduces the experimental PES spectra of sputtered surfaces.

Figure 8 shows the Cu  $3d$  PSW's of Cu-Pt alloys at  $h\nu=160$  eV obtained in this way (thin lines). Since the average atomic distance of these alloys becomes larger as the Pt content increases, the Cu  $3d$  band becomes narrow with the increasing Pt content, but on the other hand the spectral weight near the Fermi level increases due to the hybridization with the Pt  $5d$  band. The sharp structure of the Cu  $3d$  band observed in pure Cu metal disappears in the Pt-rich alloys probably due to disorder. These behaviors are similar to those in Cu-Pd alloys.<sup>25</sup>

Thick lines in Fig. 8 show the Pt  $5d$  PSW's at  $h\nu=60$  eV. As the Cu content is increased, the spectral weight of the lower binding energy structure (mainly  $5d_{5/2}$  character) is transferred to the higher binding energy structure. This behavior is as predicted by the KKR-CPA calculation,<sup>30</sup> and can be understood as a result of the mixing with the Cu  $3d$  band which is located below 2 eV. If the Pt impurity in the Cu host has its  $5d_{3/2}$  levels inside the Cu  $3d$  band and its  $5d_{5/2}$  at the top of the Cu  $3d$  band, then the  $d_{3/2}$  structure is greatly broadened due to the large hybridization caused by the compression of the Pt atomic site in the Cu host, while part of the  $d_{5/2}$  states can be pushed out of the Cu host band. The  $d_{5/2}$  structures will then be composed of the broadened part inside the Cu  $d$  band and of a peak outside, similar to the Pd partial DOS in the Cu host.<sup>24</sup>

### C. Comparison with band calculation

The comparison of these experimental PSW's for  $\text{Cu}_{50}\text{Pt}_{50}$  and  $\text{Cu}_{75}\text{Pt}_{25}$  alloys with the KKR-CPA calculations<sup>30</sup> is shown in Fig. 9, where the Fermi level of theoretical curves was shifted by 0.6 eV to align the Cu spectral features. We find that the overall bandwidth and the trend with composition are in good agreement between theory and experiment, although the KKR-CPA calculation of Ref. 30 uses the non-SCF site potentials. This is in contrast to the Ni-Pt alloy case discussed earlier (Sec. III D), where the non-SCF KKR-CPA calculation gives wrong energy positions. We can infer from this fact that the interatomic charge redistribution effect is indeed small in Cu-Pt alloys as assumed in Ref. 30.

The most noticeable discrepancy between theory and experiment is found in the high binding energy side of Pt  $5d$  states, where the experimental PSW shows small intensities compared with the theoretical DOS. This situation is similar to the case of Pd  $4d$  states in Cu-Pd alloys,<sup>21–25</sup> although not so severe. In the case of Cu-Pd alloys, a local lattice relaxation effect in alloys and the inability of the CPA calculation to include its effect were proposed as the origin of this discrepancy.<sup>42,43</sup> However, we have argued that the matrix element effect, i.e., the binding energy dependence of the photoionization cross section within the Pd  $4d$  band, is the main cause of this discrepancy rather than the local lattice relaxation effect.<sup>25</sup> We believe the same argument can be made for the Pt  $5d$  states in Cu-Pt alloys as well, since the theoretical calculation predicts a substantial change of the photoionization cross section with binding energy within the Pt  $5d$  band.<sup>44</sup>

From the Pt PSW of  $\text{Cu}_{90}\text{Pt}_{10}$ , it is clear that all of the Pt  $d$  states do not form a virtual bound state at 1.7–2 eV. Instead, most of the Pt  $5d_{3/2}$  states are located at 3–6 eV, and the total bandwidth amounts to about 6 eV. This fact calls into question the virtual bound state picture for the Pt impurity in the Cu host.<sup>22</sup> Although 10 at. % Pt is still too much to be considered as the impurity case, no drastic change of the Pt PSW is expected as the Pt concentration is lowered to 2 at. % studied in Ref. 22 for the following reasons.

It is now generally accepted that the interaction between nearest neighbors determines the electronic structures of solids for the most part, and the linear combinations of atomic

orbitals (LCAO) method with empirically determined matrix elements can give a fairly accurate description of band structures.<sup>26</sup> This is true even for many metallic systems, and the parametrized scheme devised by Harrison<sup>26</sup> has been very successful in predicting the width and position of the bands, especially for  $d$ -band metals and alloys. According to this scheme, the bandwidth is mainly determined by the hopping integral between Pt  $5d$  and Cu  $3d$  states, which in turn depends on the nearest-neighbor distance between Pt and Cu atoms. Since the lattice constant hardly changes between 10 at. % Pt alloy and 2 at. % Pt alloy, we do not expect the Pt  $5d$  bandwidth to change much from 10 at. % Pt alloy to 2 at. % alloy. If anything, the Pt  $5d$  band width will *increase* rather than decrease, since the nearest-neighbor distance becomes smaller as Pt is diluted. This is true even when the local lattice relaxation effect is included.<sup>27</sup> Hence it is highly unlikely that the Pt  $5d$  density of states suddenly shrinks to the narrow region of the binding energy around 1.7–2 eV from the total bandwidth of 6 eV when the Pt concentration is lowered from 10 at. % to 2 at. %. We therefore believe that our present work suggests the absence of the Pt virtual bound states in the Pt diluted disordered Cu-Pt alloys.

## V. CONCLUSION

In this work, we have determined the PSW's of Ni-Pt and Cu-Pt alloys by photoelectron spectroscopy using synchrotron radiation. For this purpose, we determined the cross section ratios of Ni  $3d$  and Cu  $3d$  states relative to Pt  $5d$  states experimentally and used the Cooper minimum phenomenon of the Pt  $5d$  states. We also took into consideration the surface segregation and the matrix element effect.

We found appreciable Pt spectral densities near the Fermi level of Ni-rich Ni-Pt alloys, which are believed to be the origin of the Pt local magnetic moment. The comparison with the existing band calculations of Ni-Pt alloys shows the importance of the simultaneous treatment of self-consistent field and relativistic effects.

For the Cu-Pt alloys, the experimentally determined Pt and Cu partial spectral weights are found to be in good agreement with the KKR-CPA calculation overall, although the Pt  $5d$  PSW shows some discrepancy probably because of the short lifetime and the matrix element effect. These PSW's show strong hybridization between Cu  $3d$  and Pt  $5d$  states, and suggest the absence of the Pt  $5d$  virtual bound states in the Pt-diluted Cu-Pt alloy. This is consistent with the conclusion of our previous work on the Cu-Pd alloys<sup>25</sup> that the Pd PSW in Cu-Pd alloys can be interpreted as an indication of the common-band behavior.

## ACKNOWLEDGMENTS

We thank Dr. M. Choi for providing Ni-Pt samples, and Dr. G.K. Wertheim of AT&T Bell Laboratories for his help during the experiments. This work was supported in part by



the Basic Science Research Institute Program, Ministry of Education, 1995, Project No. BSRI-95-2416, and in part by a grant from the Atomic Scale Surface Science Research Center which is sponsored by KOSEF. The travel grant to NSLS was provided by the Pohang Light Source in Korea. The

synchrotron photoemission data were obtained at the National Synchrotron Light Source, Brookhaven National Laboratory, which is supported by the Department of Energy, Division of Materials Sciences and Division of Chemical Sciences.

- \*Present address: James Franck Institute, University of Chicago, 5640 South Ellis Ave, Chicago, IL 60637.
- †Present address: AT&T Bell Laboratories, Murray Hill, NJ 07974.
- <sup>1</sup>J. Beille, D. Bloch, and R. Kuentzler, *Solid State Commun.* **14**, 963 (1974).
  - <sup>2</sup>Y. Nakai, I. Tomeno, J. Akimitsu, and Y. Ito, *J. Phys. Soc. Jpn.* **47**, 1821 (1979).
  - <sup>3</sup>R.E. Parra and J.W. Cable, *Phys. Rev. B* **21**, 5494 (1980).
  - <sup>4</sup>Y. Jugnet, J.C. Bertolini, J. Massardier, B. Tardy, T.M. Duc, and J.C. Vedrine, *Surf. Sci.* **107**, L320 (1981).
  - <sup>5</sup>J. Sedláček, L. Hilaire, P. Légaré, and G. Maire, *Surf. Sci.* **115**, 541 (1982).
  - <sup>6</sup>C.E. Dahami, M.C. Cadeville, J.M. Sanchez, and J.L. Morán-López, *Phys. Rev. Lett.* **55**, 1208 (1985).
  - <sup>7</sup>J.P. Segaud, E. Blanc, C. Lauroz, and R. Baudoing, *Surf. Sci.* **206**, 297 (1988); D. Dufayard, and R. Baudoing, *ibid.* **233**, 223 (1990).
  - <sup>8</sup>Y. Gauthier, Y. Joly, R. Baudoing, and J. Rundgren, *Phys. Rev. B* **31**, 6216 (1985); R. Baudoing, Y. Gauthier, M. Lundberg, and J. Rundgren, *J. Phys. C* **19**, 2825 (1986).
  - <sup>9</sup>Y. Gauthier, R. Baudoing, M. Lundberg, and J. Rundgren, *Phys. Rev. B* **35**, 7867 (1987); Y. Gauthier, R. Baudoing, and J. Jupille, *ibid.* **40**, 1500 (1989); Y. Gauthier, W. Hoffmann, and M. Wuttig, *Surf. Sci.* **233**, 239 (1990).
  - <sup>10</sup>J.C. Bertolini, J. Massardier, P. Delchere, B. Tardy, B. Imelik, Y. Jugnet, T.M. Duc, L. de Temmerman, C. Creemers, H. van Hove, and A. Neyens, *Surf. Sci.* **119**, 95 (1982); L. de Temmerman, C. Creemers, H. van Hove, A. Neyens, J.C. Bertolini, and J. Massardier, *ibid.* **178**, 888 (1986); L. de Temmerman, C. Creemers, H. van Hove, and A. Neyens, *ibid.* **183**, 565 (1987).
  - <sup>11</sup>S. Deckers, F.H.P.M. Habraken, W.F. van der Weg, A.W. Denier van der Gon, B. Pluis, J.F. van der Veen, and R. Baudoing, *Phys. Rev. B* **42**, 3253 (1990).
  - <sup>12</sup>J. Inoue and M. Shimizu, *J. Phys. Soc. Jpn.* **42**, 1547 (1977).
  - <sup>13</sup>J.B. Staunton, P. Weinberger, and B.L. Gyorffy, *J. Phys. F* **13**, 779 (1983).
  - <sup>14</sup>N.J. Shevchik and D. Bloch, *J. Phys. F* **7**, 543 (1977).
  - <sup>15</sup>F.J. Pinski, B. Ginatempo, D.D. Johnson, J.B. Staunton, G.M. Stocks, and B.L. Gyorffy, *Phys. Rev. Lett.* **66**, 766 (1991).
  - <sup>16</sup>P.P. Singh, A. Gonis, and P.E.A. Turchi, *Phys. Rev. Lett.* **71**, 1605 (1993).
  - <sup>17</sup>A. Pisanty, C. Amador, Y. Ruiz, and M. de la Vega, *Z. Phys. B* **80**, 237 (1990).
  - <sup>18</sup>A. Liebsch, *Phys. Rev. Lett.* **43**, 1431 (1979); *Phys. Rev. B* **23**, 5203 (1981).
  - <sup>19</sup>E. Choi, S.-J. Oh, and M. Choi, *Phys. Rev. B* **43**, 6360 (1991).
  - <sup>20</sup>P.J. Braspenning, R. Zeller, A. Lodder, and P.H. Dederichs, *Phys. Rev. B* **29**, 703 (1984).
  - <sup>21</sup>N. Mårtenson, R. Nyholm, H. Caleén, J. Hedman, and B. Johansson, *Phys. Rev. B* **24**, 1725 (1981).
  - <sup>22</sup>D. van der Marel, J.A. Julianus, and G.A. Sawatzky, *Phys. Rev. B* **32**, 6331 (1985).
  - <sup>23</sup>H. Wright, P. Weightman, P.T. Andrews, W. Folkerts, C.F.J. Flipse, G.A. Sawatzky, D. Norman, and H. Padmore, *Phys. Rev. B* **35**, 519 (1987).
  - <sup>24</sup>H. Winter, P.J. Durham, W.M. Temmerman, and G.M. Stocks, *Phys. Rev. B* **33**, 2370 (1986); N. Stefanou, R. Zeller, and P.H. Dederichs, *Solid State Commun.* **62**, 735 (1987); J. Kudrnovský and V. Drchal, *ibid.* **70**, 577 (1989).
  - <sup>25</sup>T.-U. Nahm, H. Han, S.-J. Oh, J.-H. Park, J.W. Allen, and S.-M. Chung, *Phys. Rev. Lett.* **70**, 3663 (1993); *Phys. Rev. B* **51**, 8140 (1995).
  - <sup>26</sup>W.A. Harrison, *Electronic Structure and the Properties of Solids* (Freeman, San Francisco, 1980).
  - <sup>27</sup>U. Scheuer and B. Lengeler, *Phys. Rev. B* **44**, 9883 (1991).
  - <sup>28</sup>G.G. Kleiman, V.S. Sundaram, J.D. Rogers, and M.B. de Moraes, *Phys. Rev. B* **23**, 3177 (1981).
  - <sup>29</sup>P.J. Feibelman and D.E. Eastman, *Phys. Rev. B* **10**, 4932 (1974).
  - <sup>30</sup>J. Banhart, P. Weinberger, and J. Voigtländer, *Phys. Rev. B* **40**, 12 079 (1989).
  - <sup>31</sup>J.F. Clark, F.J. Pinski, D.D. Johnson, P.A. Sterne, J.B. Staunton, and B. Ginatempo, *Phys. Rev. Lett.* **74**, 3225 (1995).
  - <sup>32</sup>J.J. Yeh and I. Lindau, *At. Data Nucl. Data Tables* **32**, 1 (1979).
  - <sup>33</sup>T.-U. Nahm, K.-H. Park, S.-J. Oh, S.-M. Chung, and G.K. Wertheim, *Phys. Rev. B* **52**, 16 466 (1995).
  - <sup>34</sup>M. Schmid, A. Biedermann, H. Stadler, and P. Varga, *Phys. Rev. Lett.* **69**, 925 (1992).
  - <sup>35</sup>G. Betz, *Surf. Sci.* **92**, 283 (1980).
  - <sup>36</sup>A.R. Williams, R. Zeller, V.L. Moruzzi, C.D. Gelatt, Jr., and J. Kübler, *J. Appl. Phys.* **52**, 2067 (1981).
  - <sup>37</sup>P. Weinberger, *J. Phys. F* **12**, 2171 (1982).
  - <sup>38</sup>David R. Penn, *Phys. Rev. Lett.* **42**, 921 (1979); G. Tréglia, F. Ducastelle, and D. Spanjaard, *J. Phys. (Paris)* **43**, 341 (1982).
  - <sup>39</sup>A.D. van Langeveld and V. Ponc, *Appl. Surf. Sci.* **16**, 405 (1983).
  - <sup>40</sup>M.J. Kelley, D.G. Schwartzfager, and V.S. Sundaram, *J. Vac. Sci. Technol.* **16**, 664 (1979).
  - <sup>41</sup>M. Schmid, A. Biedermann, H. Stadler, and P. Varga, *Phys. Rev. Lett.* **69**, 925 (1992).
  - <sup>42</sup>P. Weightmann, H. Wright, P.T. Andrews, W. Folkerts, C.F.J. Flipse, G.A. Sawatzky, D. Norman, and H. Padmore, *Phys. Rev. B* **36**, 9098 (1987).
  - <sup>43</sup>Z.W. Lu, S.-H. Wei, and A. Zunger, *Phys. Rev. B* **44**, 3387 (1991); **45**, 10 314 (1992).
  - <sup>44</sup>W. Speier, J.C. Fuggle, P. Durham, R. Zeller, R.J. Blake, and P. Sterne, *J. Phys. C* **21**, 2621 (1988).